131, 2442 (1963).
[4]D. Colman, R. T. Bate, and J. P. Mize, J. Appl. Phys. 39, 1923 (1968).
[5]F. Stern and W. E. Howard, Phys. Rev. 163, 816 (1967).
[6]F. F. Fang and A. B. Fowler, Phys. Rev. 169, 619 (1968).
[7]N. St. J. Murphy, F. Berz, and I. Flinn, Solid State Electron. 12, 775 (1969).
[8]A. Ohwada, H. Maeda, and K. Tanaka, Japan. J. Appl. Phys. 8, 629 (1969).
[9]J. R. Schrieffer, in *Semiconductor Surface Physics*, edited by R. H. Kingston (Pennsylvania U. P., Philadelphia, 1956), p. 55.
[10]C. J. Rauch, J. J. Stickler, H. J. Zeiger, and G. S. Heller [Phys. Rev. Letters 4, 64 (1960)] reported the values of $m_t = (0.192 \pm 0.001)m_e$ and $m_l = (0.90 \pm 0.02)m_e$, determined by cyclotron resonance using a wavelength of 2 mm, but no explanation was given of the discrepancy between these values of $m_l$ and $m_l = (0.98 \pm 0.04)m_e$ [G. Dresselhaus, A. F. Kip, and C. Kittel, Phys. Rev. 98, 368 (1955)].
[11]H. Sakaki, T. Hoh, and T. Sugano, IEEE Trans. Electron. Devices ED-17, 892 (1970).
[12]H. Maeda (unpublished).
[13]The sample preparation in this experiment is somewhat different from the preparation for the samples used in the main study of this paper.
[14]F. F. Fang and W. E. Howard, Phys. Rev. Letters 16, 797 (1966).
[15]T. Sugano, H. Sakaki, and K. Hoh, J. Japan. Soc. Appl. Phys. Suppl. 39, 192 (1970).
[16]F. Stern, in Proceedings of the Tenth International Conference on the Physics of Semiconductors, Cambridge, Mass., 1970, p. 451 (unpublished).
[17]E. D. Siggia and P. C. Kwok, Phys. Rev. B 2, 1024 (1970).
[18]S. Kawaji, J. Phys. Soc. Japan 27, 906 (1969).
[19]$c_n$ is the coupling constant in the $n$th subband and is given, in the triangular potential approximation, by

$$c_n = \frac{1}{2\pi}\int_{-\infty}^{\infty}\left(\frac{|\int_{-\gamma_n}^{\infty}\phi^2(\gamma)e^{-il\gamma}d\gamma|^2}{|\int_{-\gamma_n}^{\infty}\phi^2(\gamma)d\gamma|^2}\right)dl,$$

where $\phi_n$ is the Airy function and $\gamma_n$ is the $n$th root of the Airy function.
[20]H. Ezawa, T. Kuroda, and K. Nakamura, Surface Sci. 24, 654 (1971).

PHYSICAL REVIEW B VOLUME 4, NUMBER 6 15 SEPTEMBER 1971

# Exact Solutions of the Kinetic Equations Governing Thermally Stimulated Luminescence and Conductivity

Paul Kelly and M. J. Laubitz
*Division of Physics, National Research Council, Ottawa, Canada*

and

Peter Bräunlich
*Bendix Research Laboratories, Southfield, Michigan* 48075
(Received 9 April 1971)

Past analyses of the kinetic equations governing thermally stimulated luminescence and conductivity have invariably involved certain approximations; however, the validity of these approximations has never been explicitly determined. In this paper we give a procedure for determining the conditions under which the approximations are valid, and show that for a model involving a single trap depth in the presence of other deep traps, and a single type of recombination center, the validity depends critically on $N$, the number of active traps. For $N < 10^{15}$ cm$^{-3}$ the conventional approximations are inadequate, and the kinetic equations must be analyzed exactly through numerical solutions. Although no such solutions have been reported in the literature, we show that they are not only possible, but are in fact readily obtained for certain parametric ranges. Examination of these exact solutions for small $N$ reveals new features; in particular, the dependence of the processes on the density of deep traps, or on initial filling ratios of the active traps, is markedly different from the dependence at large $N$, where the approximations do hold. This invalidates, for these low densities, many approaches to the analysis of the phenomena which have been recommended on the basis of these approximations. The procedures developed here have been applied to one specific model. However, they can be readily generalized to the solutions of the equations for more complex and realistic models of solids.

## I. INTRODUCTION

Thermally stimulated luminescence (TSL) and thermally stimulated conductivity (TSC) are phenomena frequently investigated, mainly because of experimental simplicity and deceptive ease of analysis purportedly yielding useful information on the trapping parameters of solids. An early explana-

tion of one process (TSL) was given by Randall and Wilkins[1] in terms of a metastable trap from which the electrons were released at a rate proportional to the product of the number of electrons in that trap, $n$, and the factor $e^{-E/kT}$, where $E$ is the activation energy for the process, $k$ the Boltzmann constant, and $T$ the absolute temperature. This hypothesis predicted a unique temperature dependence for TSL, which, however, frequently did not correspond to that observed experimentally. The original postulates were therefore generalized, along two more or less independent paths. One arbitrarily describes both processes phenomenologically through a rate equation of the form

$$\frac{dn}{dt} = -P_0 n^c e^{-E/kT}, \tag{1}$$

where $t$ is the time, and $P_0$ and $c$ are constants, the latter not necessarily integral.[2] For $c > 2$ this equation corresponds to no physical model that we are aware of, and hence this procedure is essentially classificatory in nature, giving no insight into the physics of the process or correlations with other observable phenomena. The other approach[3-7] is to construct a physical model first, and then derive and analyze the kinetic equations for that model. One model commonly used is shown in Fig. 1; it consists essentially of $N$ traps located at a depth $E$ below the conduction band, which has a density of states $N_c$. On thermal stimulation the electrons are released from the traps into the conduction band with a probability $P = P_0 e^{-E/kT}$, from which they can either drop into empty recombination centers with a capture coefficient $\gamma$, producing TSL, or be retrapped with a coefficient $\beta$. In the absence of deep traps the rate equations for the occupation numbers in the traps and the conduction band, $n$ and $n_c$, respectively, are given by

$$\frac{dn}{dt} = -Pn + \beta n_c(N-n), \tag{2a}$$

$$\frac{d(n+n_c)}{dt} = -\gamma n_c(n+n_c). \tag{2b}$$

For $\beta = 0$ Eq. (2a) reduces to the Randall and Wilkins form, $c = 1$ in Eq. (1). For $\beta = \gamma$ Eq. (1) with $c = 2$ may be derived from Eqs. (2) if $N$ is suitably large, a condition which, as will be shown in Sec. II, ensures the validity of the so-called "approximate solutions" necessary for this derivation; for single occupation of the traps, however, there is no further immediate correspondence between the two approaches.

This second approach has a number of advantages: It is clearly related to the physics of the solid, however naive the model may be, and is thus couched in terms of parameters which can, at least in principle, be calculated theoretically or obtained from other experiments. Further, it predicts TSC if the electrons in the conduction band have any mobility at all, and correlates it with the TSL through the parameters of the model. The disadvantage of the second approach is that, whereas Eq. (1) is readily soluble, analytically or numerically, for any $P_0$, $E$, and heating program, Eqs. (2) are highly intractable, and so far have never been solved in any but an approximate way.[8] The usual approximation is based on the quite arbitrary assumptions that $n_c \ll n$ and $dn_c/dt \ll dn/dt$; solutions derived under these assumptions we shall call for convenience "approximate solutions," although strictly speaking they are exact solutions of simplified rate equations. On that basis many analyses of TSL and TSC, and correlations between them, have been described.[3-6]

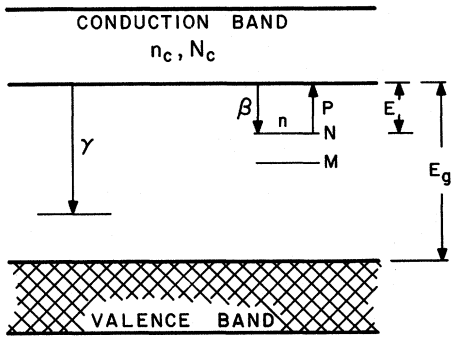


FIG. 1. Energy-level diagram forming the model analyzed in this paper.

Unfortunately the above assumptions, on which all the past work has been based, cannot be justified either physically or mathematically; indeed, on the contrary, one can show generally from Eqs. (2) that both must be violated for any set of parameters, although the critical violation involving $n$ and $n_c$ may occur at a temperature so high as to be of no physical interest. The purpose of this work is therefore to examine in detail the ranges of parameters for which the approximations, and therefore past analyses, are physically valid, to examine the regions where they are not through exact solutions of the rate equations, and compare the two, and finally, to reevaluate the usefulness of TSL and TSC, in view of this work, in providing information on the trapping parameters of solids.

Broadly speaking, what we shall show is that the approximate solutions are valid for only a part of the range of physically plausible trapping parameters; that the exact solutions lead to an even greater variability of shapes, peak positions, and magnitudes than heretofore predicted, and produce a different effect on TSL and TSC of other, thermally disconnected traps or of various initial filling ratios than do the approximate solutions; and

finally, that any analysis of TSL and TSC in the absence of extensive other information is highly unlikely to lead to unambiguous values for the trapping parameters.

## II. SOLUTIONS OF RATE EQUATIONS

### A. Approximate Solutions

To treat Eqs. (2) in detail we make a number of convenient simplifications. In the first place we convert the time derivatives into temperature derivatives through a constant heating rate $q$. We then assume that all the trapping parameters are independent of temperature, and generalize the model given above by assuming the presence of $M$ thermally disconnected deep traps (Fig. 1). The rate equations then become

$$\dot{n} = -Pn + \beta n_c(N-n) , \tag{3}$$

$$\dot{n} + \dot{n}_c = -\gamma n_c(n + n_c + M) , \tag{4}$$

where the dot indicates the temperature derivative, and $P$, $\beta$, and $\gamma$ contain implicitly the heating rate $q$. TSL is then equal to $\eta(-\dot{n}-\dot{n}_c)$ and TSC to $e\mu n_c$, where $\eta$ is the luminous efficiency, $\mu$ the mobility, and $e$ the electronic charge. The initial boundary conditions are $n = fN$, where $f$ is the initial filling ratio ($\leq 1$), and $n_c = 0$, and we further assume that $n, n_c \geq 0$, and approach zero at very large temperatures. Under these assumptions one can show generally that (i) $\dot{n} \leq 0$, (ii) $n_c$ has only one maximum at finite $T$, and (iii) $-\dot{n}-\dot{n}_c$ has only one maximum at finite $T$, which, furthermore, occurs at a lower $T$ than the maximum of $n_c$. Thus, for constant $q$, $\mu$, and $\eta$, the TSL peak always preceeds the TSC peak. One can further show in general that the TSC curve must decay more slowly than the TSL curve, and that $n_c$ must initially rise as $P/\gamma$ (which provides a useful method of determining $E$). However, the details of the shapes and peak locations cannot be obtained from general arguments, but must come from actual solutions of the equations.

In their general form the rate equations are not integrable, and so far, where numerical solutions have been obtained, these were for an approximate and not the exact version of them. The approximate version is obtained by ignoring $n_c$ relative to $n$, and $\dot{n}_c$ to $\dot{n}$, which leaves Eq. (3) unchanged, but instead of (4) produces

$$n_c = \frac{Pn}{\beta(N-n)+\gamma(n+M)} . \tag{4'}$$

The arguments used to justify this procedure are usually phrased in terms of "quasiequilibrium" and electronic lifetime in the conduction band,[6] but they are not convincing, as they lack universal validity. For instance, one can easily show from Eqs. (3) and (4) that at the start of the heating cycle $\dot{n}_c = -\dot{n}$, certainly not a negligible quantity. Furthermore, at high temperatures above the TSC peak $n_c/n \gtrsim P/(\beta N + \gamma M)$. As $P$ tends to $P_0$, which is of the order of $\beta N_c$, then for $M$ vanishing, $n_c/n \gg 1$ for any combination of the other parameters. Equally, as $M$ is at most of the order of $N_c$, this is also true for $\beta/\gamma > 1$ for any $M$. The so-called approximate solutions must therefore be inaccurate near the start, and further break down past some definite higher temperature for large ranges of the trapping parameters.

It is of course not really necessary to ignore $n_c$, relative to $n$ to decouple Eqs. (3) and (4); it is sufficient to assume $\dot{n}_c \ll \dot{n}$, which then leads to another equation for $n_c$:

$$n_c = (B/2\gamma)[(1 + 4P\gamma n/B^2)^{1/2} - 1] , \tag{4''}$$

where

$$B = \beta(N-n) + \gamma(n+M) .$$

This approach suffers from the same objection as the previous one — that initially $\dot{n}_c$ is not negligible compared to $\dot{n}$; however, this is not a serious shortcoming, for one can readily show that at the start $n_c$, the solution obtained from Eqs. (3) and (4), approaches $n_c$(b), the solution obtained from Eqs. (3) and (4′), as $e^{-\gamma N(T-T_0)}$, where $T_0$ is the starting temperature. For reasonable values the exponential vanishes rapidly and leaves no appreciable residual effect on the solution. The second approximate solution has a somewhat longer temperature range of validity, for, generally, $\dot{n}_c/\dot{n}$ is less than $n_c/n$.

The approximate solutions for $n$ and $n_c$, unlike the exact ones, can be easily obtained numerically, and have the following very useful property: If $T^*$ be the temperature of the $n_c$ peak, and the arguments $(a)$ and $(b)$ refer to the solutions obtained from Eqs. (3) and (4′) or (4″), respectively, then

$$n < n(b) < n(a), \quad n_c < n_c(b) < n_c(a), \quad T < T^* ;$$

$$n_c(b) < n_c < n_c(a), \quad n(b) < n < n(a), \quad T < T^* .$$

Above $T^*$ the approximate solutions form upper and lower bounds to the exact solutions. Below $T^*$ the exact solutions are extremal to the appropriate ones; however, in that region the differences between the exact and $(b)$ solutions can be roughly expressed as functions of $1 - \dot{n}_c(b)/\dot{n}(b)$, and the magnitude of these differences can be estimated from the computed values of $\dot{n}_c(b)/\dot{n}(b)$. It turns out that if that ratio is less than $10^{-2}$, then for practical purposes the exact and approximate solutions correspond in the region $T < T^*$.

The comparison of the approximate solutions, which (to repeat again) are easily obtained numerically, provides then a convenient method of deter-

mining the range of $T$ in which these solutions are valid approximations: The criterion is simply agreement between them to a precision required of the final solutions, and a low ratio of $\dot{n}_c(b)/\dot{n}(b)$ at $T < T^*$. Using this approach, we have examined the approximate solutions over wide ranges of some of the trapping parameters to determine the regions wherein these solutions are valid. Unfortunately, it is not feasible to perform such an investigation quite generally, for the number of possible permutations of physically meaningful parameters is uncomfortably large. We have therefore restricted our investigation to a single trapping energy, $E/k = 4000$ K, and a single density of states in the conduction band, $N_c = 10^{19}$ states/cm$^3$. We have also assumed that $P_0 = \beta N_c$, a condition that can be derived from detailed balance,[9] and we have then looked at the ranges $10^{12} \leq N \leq 10^{18}$ cm$^{-3}$, $10^{-14} \leq \beta$, $\gamma \leq 10^{-8}$ cm$^3$/K, and $M \geq 0$ cm$^{-3}$. The analyses can be readily extended to include other forms of the "frequency factor" $P_0$ and temperature dependencies of all relevant parameters, if these be known.

Under our conditions the restrictions on the parameters for which the approximate solutions are valid turned out to have a very simple form: $N_c/(N+M) \leq C$, where $C$ is a constant depending on the accuracy required of the final solution: If we are satisfied with an accuracy of the order of 1% of the peak value, then $C \sim 10^4$. For $N_c/(N+M) \sim 10$, we have found no significant difference between the approximate solutions at any temperature; if that ratio be of the order of $10^7$, the approximate solutions differ significantly from the very start.

Thus, for $M \sim 0$ the approximate solutions are valid only for a part of the physically plausible parametric ranges, i.e., for $N > 10^{15}$. For $N < 10^{15}$ the approximate solutions are invalid, and the thermally stimulated processes can only be analyzed through the exact solution of Eqs. (3) and (4). Although some previous investigators[4] have reported their inability to generate these solutions, we have actually obtained them by standard numerical procedures[10]; they will be discussed briefly in Sec. II B.

### B. Exact Solutions

The exact solutions were obtained by the Runge-Kutta-Gill fourth-order process.[10] The only difficulty, and the reason why solutions have not been obtained so far, lies in the choice of the step size $H$. To start off on the solution at all, $H$ must be less than $[\gamma(N+M)]^{-1}$, and for the solution to continue past the peak without blowing up, $H$ must also be less than $(\beta N)^{-1}$. By suitably adjusting the step size one can obtain solutions for any set of parameters; however, taking account of computer time and expense, procurement of exact solutions becomes impractical for $H < 10^{-4}$. This is actually not a severe restriction, for in general $H < 10^{-4}$ corresponds to high values of $N$, and is precisely the region wherein the approximate solutions are valid. The only corner which cannot conveniently be explored by either the exact or approximate solutions is for large $\gamma$ ($\sim 10^{-8}$) and low $N$ ($\sim 10^{12}$); fortuitously, this region is not very important for, as will be shown later, the thermally stimula-

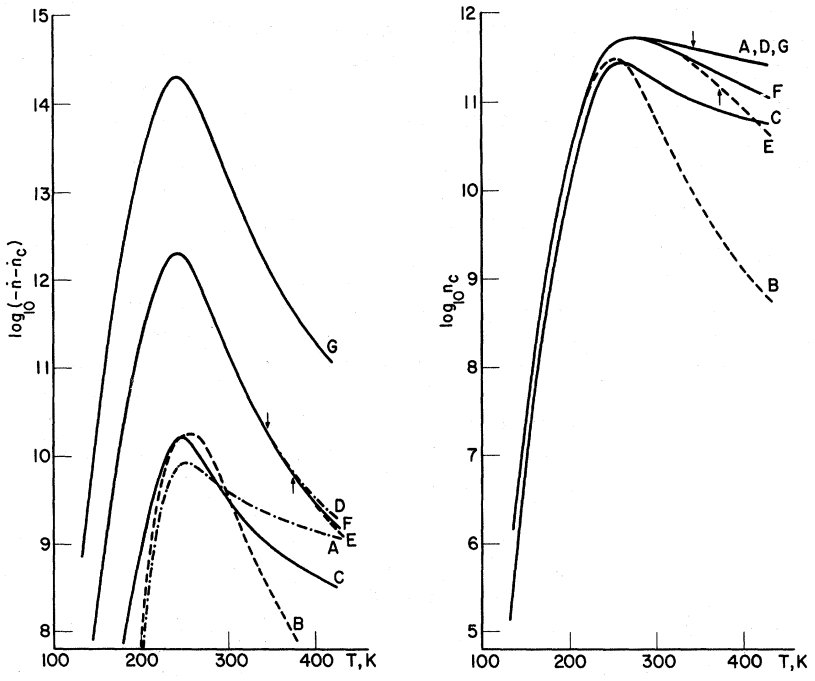


FIG. 2. Comparison of solutions of the exact and "approximate" equations, for $\beta = \gamma$, $M = 0$, and $P_0 = 10^6$ K$^{-1}$ and various $N$. Solid lines: solutions of the exact equations (3) and (4); dash-dot lines: solutions of the "approximate" equations (3) and (4′); dashed lines: solutions of the "approximate" equations (3) and (4″). $N = 10^{12}$ cm$^{-3}$ for curves A–C, $10^{14}$ for D–F, and $10^{16}$ for G, where all solutions coincide. For $n_c$ all approximate solutions of Eqs. (3) and (4′) which should be dash-dot coincide with G. Arrows on D mark position where $n_c = n$, and on E where $\dot{n}_c = \dot{n}$.

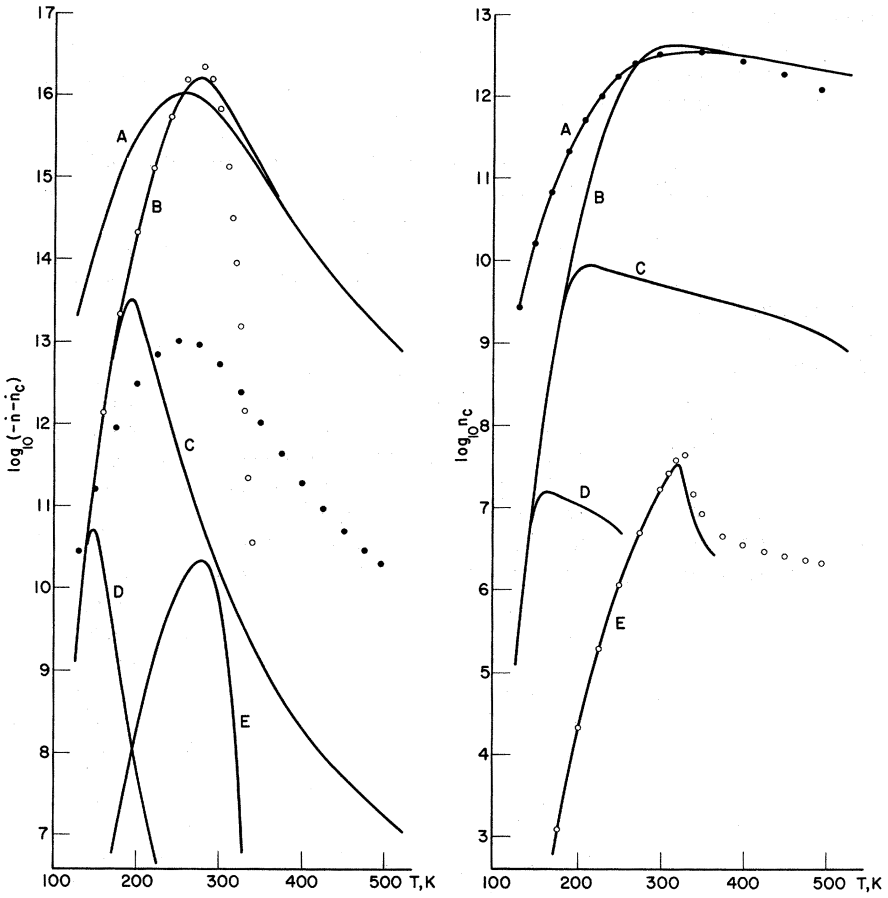


FIG. 3. Valid solutions of the kinetic equations with $M=0$, for various parameters. The ratio $\beta/\gamma$ determines the basic shape. $\beta/\gamma=10^{6}$ for A and dots, 1 for B–D, and $10^{-6}$ for E and circles. $P_0$ determines the peak position for a given shape: $P_0=10^{11}\,\mathrm{K}^{-1}$ for A, D, and dots, $10^{8}$ for C, and $10^{5}$ for B, E, and circles. $N$ determines the magnitude of $\log_{10}(-\dot{n}-\dot{n}_c)$: $N=10^{18}$ $\mathrm{cm}^{-3}$ for A, B, and circles, $10^{15}$ for C and dots, and $10^{12}$ for D and E. $\gamma^{-1}$ determines the magnitude of $\log_{10}\dot{n}_c$: $\gamma=10^{-14}\,\mathrm{cm}^3/\mathrm{K}$ for A, B, and dots, $10^{-11}$ for C, and $10^{-8}$ for D, E, and circles.

ted processes are here at their weakest, and probably barely observable.

We have therefore at our disposal methods of obtaining valid solutions for the kinetic equations for all physically meaningful ranges of parameters, by employing exact solutions for low $N$, and the approximate ones for high $N$. Figure 2 illustrates the relation among the various solutions as a function of $N$ for one particular set of parameters $\beta=\gamma$ and $M=0$. In Sec. III we will discuss briefly the valid solutions, be they exact or approximate, for various sets of parameters, and will show that the valid solutions show a marked dependence on $N$ in magnitude, peak position, and shape. This dependency, not discerned in the previous analyses, further compounds the difficulties of determining trapping parameters from the observed thermally stimulated processes.

A special case of the rate equations is that for zero retrapping, $\beta=0$. As this case does not satisfy the relation $P_0=\beta N_c$, it is not relevant to our discussion. However, it is interesting, for it is the original Randall and Wilkins case, and, when considered under the heretofore employed approximations, leads to a "first-order" TSL but an anomalous TSC, which increases monotonically with temperature.[5] The exact solution for this case is easy to obtain, and differs strikingly from the approximate one: The TSL is still first order, but the TSC exhibits a sharp peak with a broad shoulder, typical of solutions for small $\beta/\gamma$ (case E of Fig. 3). The anomaly in the TSC lies purely in the approximation, and is not contained in the original rate equations.

## III. RESULTS OF CALCULATIONS

The results that we show in this section were calculated for a constant $E$ ($E/k=4000$ K) and constant $N_c$ ($10^{19}$ states/$\mathrm{cm}^3$), as a function of $\beta$, $\gamma$, $N$, $M$, and $f$, with $P_0=\beta N_c$. Some results to be shown have already been discussed before[3–6]; however, we include them here for the sake of comparison with the new results, to illustrate the dependency on $N$, and also because of the different manner of presentation that we have adopted. Traditionally the thermally stimulated processes, and in particular TSL, have been studied in a "normalized" form. However, we feel that the magnitude of the process is important, and have illustrated the results in terms of $n$ and $n_c$. Although one may not be able to translate these numbers into actual experimental TSL and TSC curves due to

ignorance of mobility or of luminous efficiency for the particular solid in question, nevertheless, these graphs do provide an indication as to whether a process is likely to be strong or barely observable.

Figure 3 illustrates the curves for $M=0$, for a range of $\beta/\gamma$ from $10^{-6}$ to $10^{6}$, and for $N$ from $10^{12}$ to $10^{18}$ and $P_0=10^{5}$ to $10^{11}$. The curves show a great variety of shapes and a remarkable lack of correspondence between TSL and TSC. The intrinsic shape for each process is determined mainly by the ratio of $\beta/\gamma$. The peak position (for constant $E$) depends on $P_0$, although not as clearly for TSC and TSL. The striking difference between the two processes is shown in the magnitude, which for TSL is largely determined by $N$, while for TSC[11] it is proportional to $\gamma^{-1}$.

At first sight the variability and characteristic features of these curves seem to present the possibility of a ready determination of the trapping parameters from TSL-TSC correlations. However, the effects of introducing a finite $M$, shown for large $N$ in Fig. 4, largely vitiates this notion. Ridiculously small values of $M/N$ alter drastically the shape and peak position of both TSL and TSC, and, for the latter, affect strongly the magnitude as well. This is particularly true for small values of $\beta/\gamma$, so that the characteristic sharp-peaked and humped (on a logarithmic plot) TSC will probably never be seen in practice.

Most of the features shown above can be derived from analyses of the approximate solutions. In the following two graphs we show the effect of varying $N$ for various $M/N$, keeping $P_0$ and $\beta\gamma$ constant; for the approximate solutions such a variation has no effect on TSC, and merely scales the magnitude of the TSL. Figure 5 shows that $N$ not only changes the shape, peak position, and magnitude of the processes directly, but that it also modifies the influence that $M/N$ has on them; small values of $M/N$ are much more effective in influencing the thermally stimulated processes for large values of $N$ than for small ones, indicating that the absolute number of thermally disconnected traps has a bearing on the results. Figure 6 shows the influence of $N$ on the behavior resultant from various initial fillings of the traps, $f$. Here again both the variation of peak position and magnitude with $f$ depends strongly on $N$. Figures 5 and 6 indicate that conclusions derived from analyses of the approximate equations cannot be taken over into the domain of low $N$; in particular, the procedure

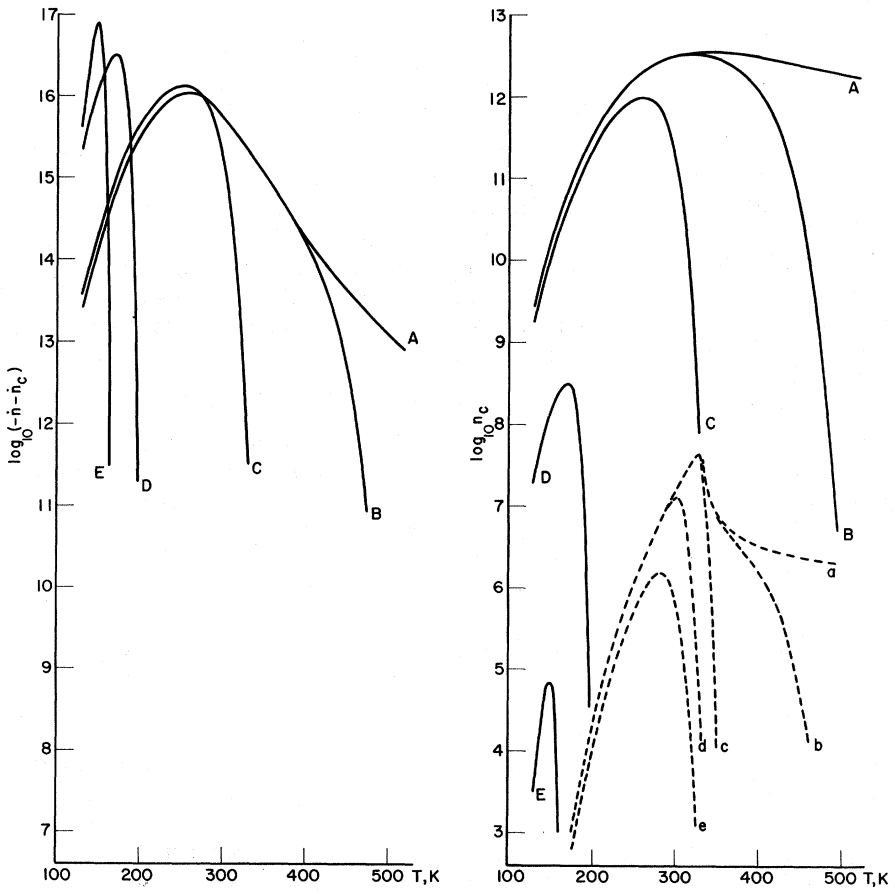


FIG. 4. Effect of the thermally decoupled deep traps $M$ on valid solutions for large $N=10^{18}\,\mathrm{cm}^{-3}$. Solid curves: $\beta/\gamma=10^{6}$, $P_0=10^{11}\,\mathrm{K}^{-1}$; curves A–E correspond to $M/N=0$, $10^{-2}$, 1, $10^{4}$, and $10^{8}$; E is physically unrealistic, and included only to show the trend. Dashed lines: $\beta/\gamma=10^{-6}$, $P_0=10^{5}\,\mathrm{K}^{-1}$; curves a–e correspond to $M/N=0$, $10^{-8}$, $10^{-6}$, $10^{-2}$, and 1, respectively; all these cases produce only a single $(-\dot{n}-\dot{n}_c)$ curve, which is shown by circles in Fig. 3, and is here excluded for clarity.

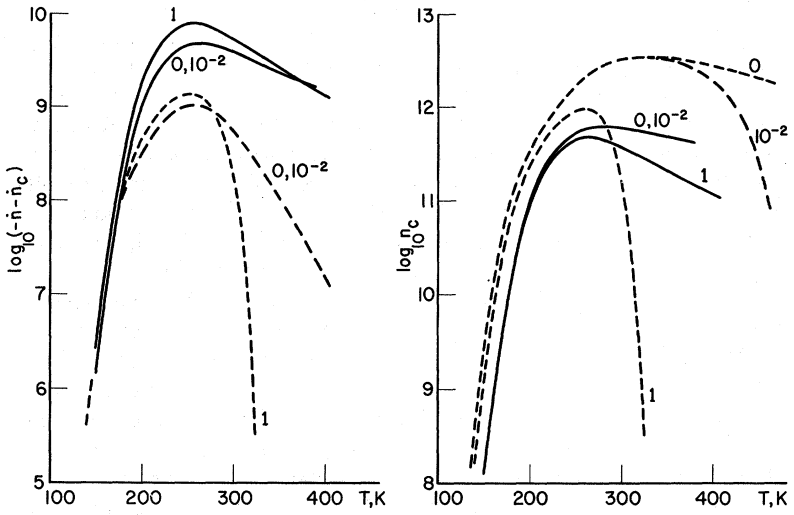


FIG. 5. Comparison of curves for small and large $N$, at $\beta/\gamma = 10^2$, $P_0 = 10^7\,K^{-1}$. Solid curves: $N = 10^{12}\,cm^{-3}$. Dashed curves: $N = 10^{18}$, where for convenience in illustration the magnitude of $(-\dot{n} - \dot{n}_c)$ has been decreased by $10^7$. Numbers near the curves give pertinent values of $M/N$.

recommended by Saunders[3] for determining the trapping parameters, by observing the effects of various $f$'s, is not nearly as unambiguous as it first appeared. In view of these findings, we must conclude that $N$ is a very important trapping parameter, influencing all of the observable properties of the thermally stimulated processes; knowledge of its magnitude is virtually indispensable to any of the phenomena.

## IV. DISCUSSION

One frequently finds in the literature statements to the effect that the study of thermally stimulated processes is an effective way of determining various trapping parameters.[12–14] Having looked hard at the problem for some time, we find such sentiments difficult to understand. Even on the basis of such a simple and naive model as the one that we have here considered, any analysis of the thermally stimulated processes is very complicated. For instance, we find that the location of the TSL and TSC peaks is a function of $P_0$, $E$, $M$, $N$, and $f$, and that their shape depends mainly on $\beta/\gamma$, $M$, and $N$; the magnitude of TSL depends on $N$, $f$, $M$ (weakly), and $\eta$, while that of TSC on $\gamma$, $M$, $N$, $f$, and $\mu$. All the observable properties depend on several parameters, of which $M$ and $N$ are common to all. As the effects of $M$ themselves depend on $N$, it is virtually impossible to interpret the experimental results uniquely if one starts from a position of complete ignorance of the parameters of the solid. The only exception to this is the trap depth $E$, which under certain conditions[3] can be obtained from "initial rise" methods; as far as we know, this is the only method independent of $N$, and therefore applicable *a priori* without the knowledge of the latter; all other methods, which are derived from the approximate solutions, such as the "half-width,"[15] "two-

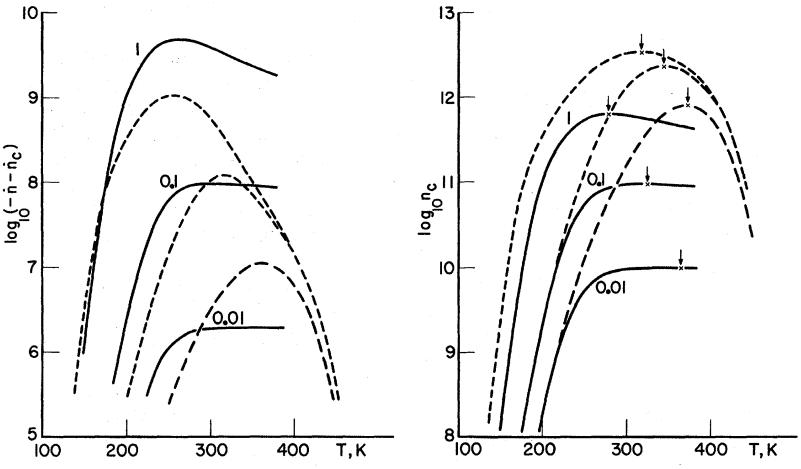


FIG. 6. Effect of initial filling for small and large $N$, at $\beta/\gamma = 10^2$, $P_0 = 10^7\,K^{-1}$, and $M/N = 10^{-2}$. Solid curves: $N = 10^{12}\,cm^{-3}$. Dashed curves: $N = 10^{18}$, where for convenience in illustration the magnitude of $(-\dot{n} - \dot{n}_c)$ has been decreased by $10^7$. Numbers near the curves give values of the initial filling ratios $f$. Arrows indicate the maxima of $n_c$.

heating-rate,"[15] or "effective-thermal-emission"[12] methods, will break down for low $N$. Having obtained $E$, however, we can proceed no further unless we know at least the luminous efficiency and the mobility; from the former and the magnitude of TSL we can calculate $N$, and from the latter we could calculate the magnitude of $n_c$, which could then be cross correlated with the shapes and peak peak positions of both TSL and TSC to yield $M$, $P_0$, $\beta$, and $\gamma$. The assumption in the foregoing is that $f$ has been determined through various initial irradiation dosages, and, of course, that each thermally stimulated process consists only of a single peak which can be determined with some accuracy over at least two orders of magnitude.

In principle, therefore, given the right conditions and some of the parameters of the solid, sophisticated experiments and analysis could yield information of the trapping parameters of the solid. The usefulness of such an approach, however, is questionable in view of the simplicity of our model; it is really too naive to expect that the low-lying levels are truly "thermally disconnected" from the conduction band, or that the trapping parameters are temperature independent.[16] One should further allow for the possibility of hole traps, as has been done by Schön,[17] for example. Under these more realistic conditions *general analyses* of the thermally stimulated processes become practically impossible, and nothing can be learned from experiments on poorly characterized solids. The inescapable conclusion is that *isolated* measurements of the thermally stimulated processes are valueless in determining the trapping parameters of the solid.

This is not to say that such analyses cannot be performed, for the difficulties most certainly are not technical; rate equations can be solved, either exactly or by means of valid approximations, through procedures analogous to those that we have here presented, for virtually any model, with any set of parameters. For example, we have obtained exact numerical solutions for models as disparate as those of Schön,[17] where hole traps coexist with electron traps, and of Bräunlich,[18] which predicts "negative" TSC. Equally, the rate equations can be solved, and TSL and TSC calculated, for any arbitrary temperature dependence of the various parameters; the artificial simplifications used heretofore in this field are neither necessary nor useful, for they lull one into a false sense of simplicity. The real problem of analysis is that unless the model applicable to the solid in question is known beforehand, any particular process can be analyzed in a large variety of ways, each of which will yeild different values for the pertinent parameters. For instance, the broad curves A of Fig. 3 can be analyzed in terms of our model, or a model with two closely spaced sets of electron traps, which produce two overlapping peaks, or a set of hole traps and a set of electron traps, or sets of traps at discrete energies, or traps with continuous energy distributions, and this list can be continued *ad infinitum*. From the view point of isolated experiments any of these explanations are equally probable, and their sum total not very informative.

As a consequence we are convinced that analyses of thermally stimulated processes can only be meaningful if the defect structure of the solid is known, so that a realistic model may be constructed, and if some of the associated parameters, such as mobility and luminous efficiency, as well as the band structure, are reasonably well known as functions of temperature. Then, and only then, will analyses of TSC and TSL provide useful and unambiguous information of the trapping parameters.

---

[1]J. T. Randall and M. H. F. Wilkins, Proc. Roy. Soc. (London) A184, 366 (1945).

[2]C. E. May and J. A. Partridge, J. Chem. Phys. 40, 1401 (1964).

[3]I. J. Saunders, J. Phys. C 2, 2181 (1969).

[4]P. Kelly and P. Bräunlich, Phys. Rev. B 1, 1587 (1970).

[5]P. Bräunlich and P. Kelly, Phys. Rev. B 1, 1596 (1970).

[6]G. A. Dussel and R. H. Bube, Phys. Rev. 155, 764 (1967).

[7]A. Halperin and A. A. Braner, Phys. Rev. 117, 408 (1960).

[8]Exact solutions for constant temperature have been published by R. C. Herman, C. F. Meyer, and H. S. Hopfield, J. Opt. Soc. Am. 38, 999 (1948); P. Kelly and P. Bräunlich, Phys. Rev. B 3, 2090 (1971).

[9]J. S. Blakemore, *Semiconductor Statistics* (Pergamon, New York, 1962), pp. 180–183.

[10]A. Ralston and H. S. Wilf, *Mathematical Methods for Digital Computers* (Wiley, New York, 1965), Vol. 1, pp. 110–120.

[11]This fact presents a potentially useful method of determining $\gamma$. One can show generally from Eqs. (3) and (4) that at the TSL peak, for constant $\eta$, the following relation holds: $\dot{n}_c = \gamma n_c^2$. Thus, if $\rho = (e\mu n_c)^{-1}$, then $\dot{\rho} = (e\mu)^{-1}(\gamma + \mu/n_c\mu)$. Knowledge of the mobility, therefore, permits the determination of $\gamma$ from the slope of the thermally stimulated resistivity curve at the TSL peak.

[12]P. S. Pickard and M. V. Davis, J. Appl. Phys. 41, 2636 (1970).

[13]P. J. Kemmey, P. D. Townsend, and P. W. Levy, Phys. Rev. 155, 917 (1967).

[14]M. E. Haine and R. E. Carley-Read, J. Phys. D 1, 1257 (1968), and references therein.

[15]P. J. Kelly and M. J. Laubitz, Can. J. Phys. 45, 311 (1966). In retrospect, this paper constitutes a prime example of how not to analyze thermally stimulated pro-

cesses.

[16]One can obtain an indication of the temperature dependency of the parameters through decay studies at constant $T$. Decay, for constant parameters, yields no information which is not already contained in the TSL and TSC curves; if the parameters are temperature dependent, however, then the decay pattern will be inconsistent with the presumed (constant) parametric description of the curves, and thus will provide a warning that the assumed model is too simple.

[17]M. Schön, Tech. Wiss. Abhandl. Osram-Ges. 7, 175 (1958).

[18]P. Bräunlich, J. Appl. Phys. 39, 2953 (1967).

PHYSICAL REVIEW B VOLUME 4, NUMBER 6 15 SEPTEMBER 1971

# Electron Paramagnetic Resonance of the Neutral ($S$=1) One-Vacancy–Oxygen Center in Irradiated Silicon†

K. L. Brower
*Sandia Laboratories, Albuquerque, New Mexico* 87115
(Received 10 August 1970)

A new EPR spectrum, labeled Si-$S1$, has been observed in electron- or neutron-irradiated, $n$- or $p$-type, crucible-grown silicon under illumination with approximately band-gap light. The Si-$S1$ spectrum consists primarily of a fine-structure spectrum and a $^{29}$Si hyperfine spectrum. By incorporating $^{17}$O atoms into vacuum-float-zone silicon by ion implantation, the Si-$S1$ $^{17}$O hyperfine spectrum was also observed. An analysis of the coupling tensors in the spin Hamiltonian which characterize the fine structure and $^{29}$Si hyperfine spectrum is presented and suggests that the Si-$S1$ center is the neutral charge state of the one-vacancy–oxygen center in an excited spin-triplet state. This model for the Si-$S1$ center is in agreement with stress measurements, which are also presented. These measurements indicate that the time-temperature dependence in the reorientation of the Si-$S1$ center is the same as that of the neutral one-vacancy–oxygen center as monitored by the Si-$B1$ spectrum.

## I. INTRODUCTION

Previous studies have shown that the dominant paramagnetic centers that are formed in electron-irradiated, crucible-grown silicon at room temperature are the Si-$B1$ center[1–4] and the Si-$G15$ (oxygen-associated) center.[5–6] The Si-$B1$ center was previously identified[1–4] as the negative charge state of the one-vacancy–oxygen center. Recently it has been shown that these centers also exist in low-fluence fast-neutron-irradiated crucible-grown silicon.[7] In looking at irradiated silicon samples under illumination with electron paramagnetic resonance (EPR), we have found a new spin-1 spectrum, labeled Si-$S1$, which is prevalent in $n$- and $p$-type, electron- or neutron-irradiated, crucible-grown silicon. The Si-$S1$ spectrum is also observed in some samples of LOPEX and vacuum-float-zone silicon, but the intensity of the spectrum is less than that observed in crucible-grown silicon by at least a factor of 20. In this paper we report many of the outstanding features that are observed in the Si-$S1$ spectrum. A detailed analysis of the Si-$S1$ spectrum is presented and indicates that the Si-$S1$ center is the neutral one-vacancy–oxygen center in an excited spin-triplet state.

The electronic and molecular structure of the Si-$S1$ center is deduced from an unusually rich EPR spectrum. Section II discusses briefly the experimental aspects of the EPR measurements. The analysis of the Si-$S1$ spectrum in Sec. III deals with the development of the appropriate spin Hamiltonian, the constraints on the coupling tensors in this spin Hamiltonian, and the numerical analysis and values for the coupling tensors as deduced from the Si-$S1$ spectrum. An analysis of the coupling tensors in terms of the physical interactions which they represent is presented in Sec. IV and shows how the structure of the Si-$S1$ center evolves from this analysis. We have also succeeded in correlating the Si-$S1$ center with the Si-$B1$ center through the time-temperature dependence in the reorientation of these centers.

## II. EXPERIMENT

The samples used in the study of the Si-$S1$ center were crucible-grown $n$-type silicon (P-doped, 0.04–10 Ω cm) and $p$-type silicon (B-, Al-, or Ga-doped, 0.7–5 Ω cm). These samples were irradiated at room temperature with 2-MeV electrons with fluences up to $3\times10^{17}$ $e/\mathrm{cm}^2$. The spectrum of the Si-$S1$ center which is seen in $n$- or $p$-type, electron-irradiated, crucible-grown silicon for $\vec{H} \parallel [110]$ is shown in Fig. 1. The Si-$S1$ center is also observed in neutron-irradiated crucible-grown silicon for fluences $\lesssim 10^{17}$ $n/\mathrm{cm}^2$. The Si-$S1$ spectrum was also observed in some samples of